

Coordination Properties of Dithiobutylamine (DTBA), a Newly Introduced Protein Disulfide Reducing Agent

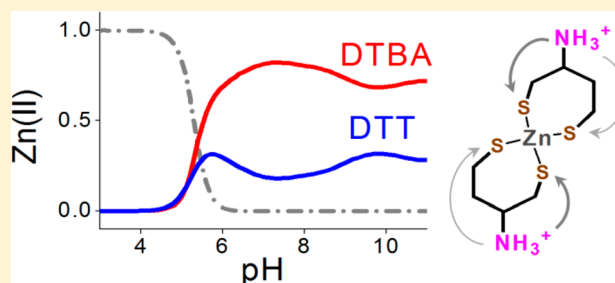
Justyna Adamczyk,[†] Wojciech Bal,[‡] and Artur Krężel^{*†}

[†]Laboratory of Chemical Biology, Faculty of Biotechnology, University of Wrocław, Joliot-Curie 14a, 50-383 Wrocław, Poland

[‡]Institute of Biochemistry and Biophysics, Polish Academy of Sciences, Pawinskiego 5a, 00-106 Warsaw, Poland

S Supporting Information

ABSTRACT: The acid–base properties and metal-binding abilities of (2*S*)-2-amino-1,4-dimercaptobutane, otherwise termed dithiobutylamine (DTBA), which is a newly introduced reagent useful for reducing protein and peptide disulfides, were studied in solution using potentiometry, ¹H NMR spectroscopy, spectropolarimetry, and UV–vis spectroscopy. The list of metal ions studied here includes Zn(II), Cd(II), Ni(II), Co(II), and Cu(I). We found that DTBA forms specific and very stable polynuclear and mononuclear complexes with all of these metal ions using both of its sulfur donors. DTBA forms complexes more stable than those of the commonly used disulfide reducing agent DTT, giving it more interference capacity in studies of metal binding in thiol-containing biomolecules. The ability of DTBA to strongly bind metal ions is reflected in its limited properties as a thiol protectant in their presence, which is manifested through slower disulfide reduction kinetics. We found that this effect correlated with the stabilities of the complexes. Additionally, the reducing properties of DTBA toward MMTS-modified papain (MMTS = S-methylmethanethiosulfonate) were also significantly affected by the investigated metal ions. In this case, however, electrostatic interactions and stereospecific effects, rather than metal-binding abilities, were found to be responsible for the reduced protective properties of DTBA. Despite its limitations, a high affinity toward metal ions makes DTBA an attractive agent in competition studies with metalloproteins.



INTRODUCTION

(2*S*)-2-Amino-1,4-dimercaptobutane, which can be shortened to dithiobutylamine (DTBA, CAS Registry Number 1363376-98-0), is a newly introduced reagent recommended for the protection of thiol groups in proteins.^{1,2} Currently, this role is largely played by Cleland's reagent, dithiothreitol (DTT, racemic (2*S*,3*S*)-1,4-dimercaptobutane-2,3-diol),³ tris(2-carboxyethyl)phosphine (TCEP),⁴ bis(2-mercaptoethyl)sulfone (BMS),⁵ and β -mercaptoethanol (β ME).⁶ The inventors of DTBA sought a compound that would react with disulfides faster than commonly used DTT, which reacts sluggishly with protein thiols at neutral pH, which is caused by the high basicity of DTT thiols, with pK_a values of 9.0 and 10.0.^{7–9} Therefore, a compound with thiol groups more acidic than those of DTT was needed. DTBA is a molecule closely related to DTT, differing by the absence of two hydroxy groups, one of which is replaced by an amino group (Figure 1). The presence of a positively charged amino group in a mercaptan molecule (e.g., cysteamine) increases thiol group acidity due to inductive effects.¹⁰ Indeed, the pK_a values of DTBA thiols determined in the original report (8.2 and 9.3) were nearly one logarithmic unit lower than those of DTT.¹ As expected, at acidic and neutral pH, DTBA reacted with low molecular weight disulfides faster than DTT. It was also more efficient in restoring the enzymatic function of oxidized thiol

proteins.¹ An additional advantage of DTBA is its chirality, enabling its application in stereospecific reactions.

The biochemistry of many metal ions, both essential and toxic, is controlled by interactions with low molecular weight thiols and thiol proteins. Prominent examples include glutathione, thioredoxin, and metallothioneins.^{11–15} Conversely, thiol-containing proteins such as zinc fingers, metal ion transporters, and thiol proteases are frequent targets of metal toxicity.^{16–19} Selective protection of thiol groups in experiments including thiol proteins and metal ions is therefore of importance in biochemical studies. DTT is a very strong and nonspecific metal ion chelator, forming a range of polynuclear complexes.^{7,20–22} This makes it a useful, albeit difficult to use, competitor for the determination of binding constants of metal ion–thiol protein complexes but rather useless in other assays involving heavy metal ions. Non-thiol disulfide reductants with significantly lower affinity for metal ions, a prominent example being TCEP, have been used in this respect,²³ with successes interacting with relatively small molecules up to zinc finger peptides and metallothioneins.^{15,24–28} The efficacy of TCEP in the protection of larger proteins, however, proved to be limited. Moreover, TCEP can cause cysteine desulfurization at elevated temperatures.²⁹

Received: October 17, 2014

Published: December 22, 2014

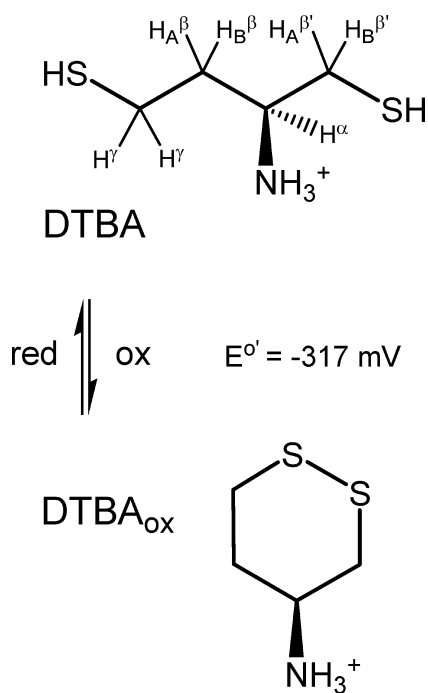


Figure 1. Structures of DTBA in its reduced (DTBA) and oxidized (DTBA_{ox}) forms. E° is the standard redox potential.¹

We studied the coordination properties of DTBA toward several metal ions that are known to bind strongly to thiol groups and to have biological significance. Among these metal ions, Zn(II) and Cu(I) form physiological thiolate complexes (e.g., at catalytic, structural, regulatory, or transport sites in dedicated proteins). Ni(II), Co(II), and Cd(II) ions may exert toxicity by interfering with these complexes and free thiol groups. Understanding the properties of DTBA complexes with these ions is important if DTBA is to be used to protect metal-binding proteins from oxidation. Only detailed knowledge of the metal-binding properties may help to avoid conditions that enable the withdrawal of metal ions from their protein binding sites by DTBA, thus acting as an unwanted competitor. Such knowledge may also lead to its application as a designated competitor in determinations of metal-binding constants of proteins, as is now the case for DTT.^{30,31}

EXPERIMENTAL SECTION

Materials. (2*S*)-2-Amino-1,4-dimercaptobutane (dithiobutylamine, DTBA), HEPES, 3-(trimethylsilyl)-1-propane-sulfonic-*d*₆ acid sodium salt (TSP), *S*-methylmethanethiosulfonate (MMTS), lyophilized papain from papaya latex, *N*_ε-benzoyl-*D,L*-arginine *p*-nitroanilide hydrochloride (BApNA), 5,5'-dithiobis(2-nitrobenzoic acid) (DTNB), ZnCl₂, ZnSO₄·7H₂O, NiCl₂·6H₂O, CuCl₂·2H₂O, CoCl₂·6H₂O, Co(NO₃)₂·6H₂O, CdCl₂, ²H₂O (99.99%), HNO₃ (redistilled 70%; 99.999% trace metal basis), 70% HClO₄, and NaOH volumetric solutions were purchased from Sigma-Aldrich. Cd(NO₃)₂·4H₂O, NaClO₄·H₂O, and KCl were obtained from Merck. NaCl, 37% HCl from POCH, Chelex 100 from Bio-Rad, and ²HCl (20% w/w) was obtained from Cambridge Isotope Laboratories.

Synthesis and Purification of Oxidized DTBA (DTBA_{ox}). DTBA (0.1 g) was dissolved in 10 mL of Milli-Q water, and the pH was adjusted to 9.5 with 2 M NaOH. To oxidize DTBA, the solution was bubbled with air constantly and was frequently readjusted to maintain the pH at 9.5. The concentration of thiol groups was monitored every 2 h by Ellman's test with DTNB.³² The reaction was carried out until thiol oxidation was complete (within 12 h). The solution was then evaporated to dryness, and a solid was purified by

HPLC (4 mL/min) with water in 0.1% TFA (v/v) over 4 min, followed by a linear gradient (0–30% v/v) of acetonitrile in 0.1% (v/v) TFA over 30 min using a Waters 1525 system with a C18 Phenomenex Gemini-NX column (110 Å, 250 × 10.00 mm). The cyclic product of the reaction, DTBA_{ox}, was identified using ESI-MS (Applied Biosystems). The calculated *m/z* value for [C₄H₉NS₂H]⁺ (M + H⁺) was 136.0; found, 136.1.

Potentiometry. Protonation constants of DTBA and stability constants of its metal complexes were measured in the presence of 0.1 M KNO₃ at 25 °C using pH metric titrations over the pH range of 2.5–11.0 (Molspin automatic titrator) with 0.1 M NaOH as the titrant. The single protonation constant of DTBA_{ox} was measured under identical conditions. Changes in pH were monitored with a combined glass–Ag/AgCl microelectrode (Biotrode, Methrom) calibrated daily in hydrogen concentrations by HNO₃ titrations.³³ Sample volumes of 2.0 mL, DTBA concentrations of 1.5 mM, and 4:1–7:1 ligand/metal ratios were used. The data were analyzed using the SUPERQUAD program.³⁴ Standard deviations computed by SUPERQUAD refer only to random errors.

Electronic Absorption (UV–Vis). Absorbance spectra were recorded on a Jasco V-650 spectrophotometer in the spectral range of 200–800 nm in 1.0 cm cuvettes. The spectra were recorded in 0.1 M NaClO₄ at 25 °C over the pH range of 3.5–12.5 by manually adding small amounts of concentrated HClO₄ or NaOH solution. The spectra of deoxygenated samples were recorded using 100 μM DTBA and 25 μM Zn(II), Cd(II), Ni(II), or Co(II). In the case of Cu(I), 300 μM DTBA and 75 μM Cu(II) were initially mixed at pH 3.5. The final content of the Cu(I)–DTBA samples (after Cu(II) reduction) was 75 μM Cu(I), 262 μM DTBA, and 37.5 μM DTBA_{ox}, assuming a 1:2 ligand/metal reaction stoichiometry, on the basis of the redox balance. Each spectrum was recorded for a fresh sample (initial pH ~3.5) with the pH adjusted directly before measurements to minimize thiol oxidation during sample manipulations. The pH* values (readings in ²H₂O of a pH meter calibrated with standard buffers in H₂O) of samples prepared in ²H₂O were adjusted using 5 M ²HCl or 3 M NaOH in ²H₂O and then converted to pH values according to a previously reported formula (eq 1).³⁵ The absorbance of DTBA measured at 233 (H₂O) and 231 nm (²H₂O) was fitted to a two-step binding model using Origin 8.6 software.

$$\text{pH} = \text{pH}^* \times 0.932 + 0.42 \quad (1)$$

Circular Dichroism (CD). CD spectra were recorded on a J-815 spectropolarimeter (Jasco) in the spectral range of 250–400 nm and the pH range of 6–12.3 in 1.0 cm cuvettes. DTBA solutions (3 mM) were prepared initially in 0.1 mM NaClO₄ at pH ~5.0 and then deoxygenated with nitrogen. All spectra were measured at 25 °C under a well-controlled N₂ atmosphere. Temperature was controlled by a Peltier heating/cooling system. Five accumulations of each spectrum were averaged using the 5 nm bandwidth, 200 nm/min scanning speed, and 1.0 nm spectral interval. Background subtraction was carried out for all spectra using similar parameters. The ellipticity of DTBA measured at 283 nm was fitted independently to a one- or two-step binding model using Origin 8.6 software (eqs 2 and 3).

$$\theta = \frac{\theta_p H^n + \theta_u K_1^n}{H^n + K_1^n} \quad (2)$$

$$\theta = \frac{\theta_p H^2 + \theta_i K_1 H + \theta_u K_1 K_2}{H^2 + K_1 H + K_1 K_2} \quad (3)$$

where θ , θ_p , θ_i , and θ_u denote the observed ellipticity and the ellipticity of protonated, intermediate, and unprotonated states, respectively; H and n correspond to the concentration of H⁺ ions and Hill's coefficient, respectively; and K_1 and K_2 are dissociation constants.

NMR Spectroscopy. ¹H NMR spectra were recorded on a Bruker AMX-300 spectrometer at 300 MHz. The spectra were expressed in δ (ppm) relative to TSP, which was used as an internal standard. The acidity of NMR samples was measured in pH* units and subsequently converted to pH values using eq 1. To avoid oxidation, a 10 mM ²H₂O

solution of DTBA at pH 5 was deoxygenated, followed by adjusting the pH to the desired level using either 2 M ^2HCl or 2 M NaOH in $^2\text{H}_2\text{O}$. All samples with metal ions were prepared similarly with 4:1 molar ratios of DTBA to M^{n+} . All manipulations were performed under a nitrogen atmosphere. The spectra were recorded at 25 °C within 2 h of preparation. Chemical shifts of all protons of DTBA were fitted independently to one- and two-step binding models (eqs 2 and 3, substituting ellipticities with chemical shifts) using Origin 8.6 software.

Elemental Analysis. Polynuclear M^{n+} -DTBA complexes were obtained in a water solution under appropriate conditions for each metal ion taken from potentiometric data simulations. Briefly, 0.2 mmol of DTBA was dissolved in 8 mL of Milli-Q water, and the pH was adjusted to 5.0 (Zn(II)), 4.0 (Cd(II)), 4.5 (Ni(II)), 5.5 (Co(II)), or 3.5 (Cu(I)) under nitrogen. Subsequently, 0.09 mmol of the respective metal ion chloride was added to the solution, and the pH was again adjusted to the values listed above. Precipitates were centrifuged at 3000g, and pellets were resuspended in Milli-Q water. Washing with water was repeated three times in order to obtain pure polynuclear complexes. Solids were dried at 65 °C overnight. The analyses of carbon, nitrogen, hydrogen, and sulfur contents of dry precipitates were performed on a Vario EL III elemental analyzer (Elementar Analysensysteme GmbH).

Papain Modification. Commercial papain from papaya latex was modified with MMTS according to a previous study with minor modifications.¹ Briefly, a solution of MMTS was prepared by dilution of 3 μL of MMTS ($\geq 98\%$) with 1 mL of 0.1 M potassium phosphate buffer pH 7.0 containing 2 mM EDTA and 0.15 M KCl. The solution was deoxygenated with nitrogen for 15 min. Then, 30 mg of papain was added, and the resulting solution was incubated at room temperature overnight under nitrogen. The modified (oxidized) papain was separated from excess MMTS by size-exclusion chromatography using a Sephadex G-25 column equilibrated with 0.1 M HEPES at pH 7.0. The final concentration of protein was determined spectrophotometrically at 280 nm using $\epsilon_{280} = 56000 \text{ M}^{-1} \text{ cm}^{-1}$. All buffers were treated with Chelex 100 prior to use to minimize the presence of heavy metal ions.

Papain Activity Assay. Activation of oxidized papain by DTBA and its metal ion complexes was analyzed spectrophotometrically with BApNA as a substrate. The 50 μM solutions of purified, oxidized papain were mixed with DTBA or its complexes (4:1 ligand/metal ratio) in 0.1 M HEPES at pH 7.0 to a final concentration of 100 μM DTBA. The total volume of each reaction mixture was typically 350–550 μL . In the case of the Cu(I)-DTBA complex, a higher concentration of ligand was used (112.5 μM) due to its partial oxidation of DTBA through its reaction with Cu(II). The 100 μL aliquots of the mixture were transferred at desired time points to a cuvette that contained 900 μL of 1.25 mM BApNA in 0.10 M HEPES at pH 6.0. Initial concentrations of DTBA (DTBA_0) and the inactive enzyme (P_0) were 10 and 5 μM , respectively. The absorbance increase was monitored at 410 nm at 25 °C over 2–5 min and fitted to the linear equation to obtain the rate of the reaction. All kinetic measurements were performed in triplicate and analyzed using standard analysis software. To calculate the second-order rate constant k_{obs} for the different metal ions, enzyme activities (reaction rates) were normalized to the 0–100% range and then fitted to eq 4.¹

$$\text{Normalized Rate} = \frac{\text{DTBA}_0 - \text{DTBA}_0 e^{k_{\text{obs}}(P_0 - \text{DTBA}_0)}}{\text{DTBA}_0 - P_0 e^{k_{\text{obs}}(P_0 - \text{DTBA}_0)}} \times 100\% \quad (4)$$

DTNB Reduction by DTBA Complexes. The influence of heavy metal ions on DTNB reduction was studied spectrophotometrically. Cuvettes with freshly prepared 100 μM DTNB solutions in 50 mM HEPES at pH 7.4 were blanked at 412 nm, and then small aliquots of 2 mM DTBA or its complexes with metal ions (4:1 ligand/metal ratio) were added to a final concentration of 10 μM DTBA and 2.5 μM metal ion. In the case of Cu(I)-DTBA, a higher concentration of ligand (11.25 μM) was used to obtain the final concentration of 10 μM DTBA after Cu(II) reduction. The reduction of DTNB was monitored

at 412 nm over 10 min. All kinetic experiments were performed in triplicate, and the data were averaged.

RESULTS

The DTBA molecule contains three protonating groups: two chemically inequivalent thiols and one amine. Dissociation constants of these groups were measured using four different techniques: potentiometry, spectrophotometry, spectropolarimetry, and ^1H NMR spectroscopy. These techniques differ in terms of numerical accuracy. Potentiometry is the best among them in this respect, but the information it provides has a global and indirect character. As such, it cannot provide group-specific assignments of protonation events. Therefore, we used the pK_a values derived from potentiometry to calculate the pH distribution of molar fractions of individual protonic forms of DTBA (Figure 2). Results from other techniques were used to

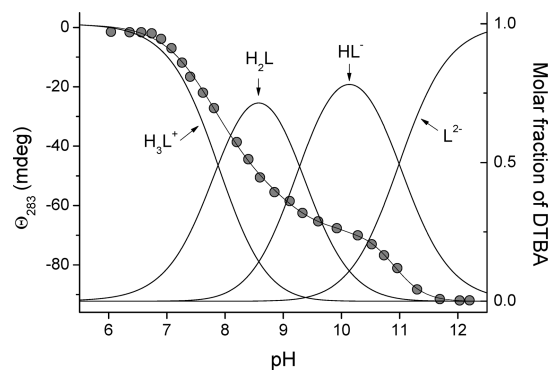


Figure 2. Comparison of spectropolarimetric pH titration of 3.0 mM DTBA in 0.1 M NaClO_4 at 25 °C with the molar fraction distribution plotted using potentiometric protonation constants. Ellipticity changes were measured at 283 nm.

confirm these data and to establish acidities of individual functional groups of this molecule. All pK_a values obtained by various techniques are provided in Table 1. The spectropolarimetric titration of DTBA confirmed all three protonation events obtained from potentiometry, which is clearly seen in the titration curve overlaid on the potentiometric plot in Figure 2. The spectrophotometric titration in the UV spectral range allowed us to determine the dissociation constants of the thiols in the DTBA molecule because the amine group is spectroscopically silent in the available UV range. The wavelength used for monitoring was 233 nm. Absorbance plotted against pH exhibited an inflection point that is characteristic of a significant difference in the acidities of the thiols (>1.5 log units, Figure S1, Supporting Information (SI)). Although the amine group does not absorb in this range, we were able to determine its dissociation constant by analyzing the maximum band shift at basic pH. The value of pK_{a3} was found to be 11.08, which correlates well with potentiometric and CD data (Figure S2, SI). Finally, ^1H NMR spectroscopy was used for unambiguous assignments. pH-dependent monitoring of the chemical shifts is shown in Figure 3. Constants presented in Table 1 are averaged values of dissociation constants derived from chemical shift changes of individual DTBA protons (Table S1, SI). An additional spectrophotometric titration was performed in $^2\text{H}_2\text{O}$ (monitored at 231 nm) to obtain a direct comparison of spectrophotometric and NMR results (Figure S3, SI). Dissociation constants determined in both solvents are

Table 1. Dissociation Constants of DTBA and DTBA_{ox} As Determined by Potentiometry, UV–Vis,^a CD, and ¹H-NMR Titration at 25 °C and I = 0.1 M

technique	DTBA			DTBA _{ox}
	pK _{a1}	pK _{a2}	pK _{a3}	pK _{a1}
potentiometry	7.88 ± 0.01 ^b	9.28 ± 0.01 ^b	10.999 ± 0.006 ^b	
UV–vis (H ₂ O)	7.76 ± 0.01	9.31 ± 0.01	11.08 ± 0.04	
UV–vis (² H ₂ O)	7.82 ± 0.07	9.23 ± 0.07	^c	
CD	7.83 ± 0.08	9.11 ± 0.24	10.90 ± 0.03	
¹ H NMR	7.81 ± 0.06	9.28 ± 0.16	10.98 ± 0.04	8.60 ± 0.04
average	7.82 ± 0.05	9.25 ± 0.09	10.99 ± 0.05	

^aValues determined spectrophotometrically were obtained for DTBA titrations in H₂O and ²H₂O. ^bDerived from cumulative constants determined directly from potentiometric data analysis: log β_{HL} = 10.999 ± 0.006, log β_{H₂L} = 20.277 ± 0.005, and log β_{H₃L} = 28.157 ± 0.006, according to pK_a = log β_{H_nL} – log β_{H_{n-1}L}. ^cThe pH* range used in the experiment allowed us to determine only the first two values.

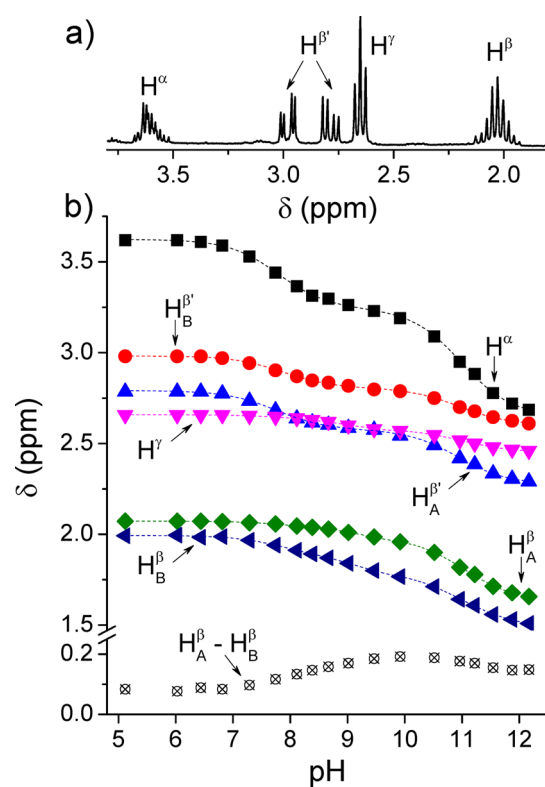
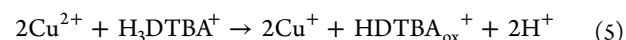


Figure 3. (a) ¹H NMR spectrum of 10 mM DTBA in ²H₂O at pH 5.12 and 25 °C with proton assignments listed. (b) pH dependence of chemical shifts. Dashed lines depict fits assuming all dissociation events. H^β_A and H^β_B correspond to differential chemical shifts of H^β_A and H^β_B protons, respectively.

convergent, as listed in Table 1. These careful experiments allowed us to conclude that the first dissociation constant (pK_{a1}) of DTBA is ~0.4 log unit lower than reported previously.¹

Although DTBA solutions were degassed, and the samples were placed in NMR tubes under a nitrogen atmosphere and were measured within 1–2 h, oxidation of DTBA was observed above pH 7. This resulted in a new set of signals in the ¹H NMR spectra, which could be assigned to cyclic disulfide DTBA_{ox}. We used this opportunity to establish acid–base properties of this molecule. Because both sulfur atoms formed a disulfide bond, the amine was the only remaining protonating group in DTBA_{ox}. It is significantly more acidic (pK_a = 8.60) compared to the amine of DTBA (pK_a = 10.98) (Figure S4, SI).

Table 2 provides stability constants of metal ion complexes of DTBA obtained from potentiometry. Similar to DTT, DTBA complexes exhibited a tendency to precipitate at ligand/metal ratios lower than 4:1 at slightly acidic to neutral pHs.⁷ To avoid precipitation, ratios between 4:1 and 7:1 were used in all titrations. Excess ligand relative to the metal ions did not pose a problem in data analysis because all of the metal ions formed highly stable complexes at acidic (Cu(I), Cd(II), Zn(II)) and neutral pHs (Ni(II), Co(II)). Therefore, metal ion-induced deprotonations of DTBA did not overlap with spontaneous deprotonation events of the uncoordinated ligand that occur in the basic pH range. The addition of Cu(II) to the DTBA solution at pH ~2.5 (the starting point of all pH titrations) resulted in the immediate, full reduction of Cu(II) to Cu(I) by an equivalent amount of DTBA, which was converted to DTBA_{ox} (eq 5).



This fact was taken into consideration during potentiometric data analysis by reducing the initial concentration of DTBA and

Table 2. Stability Constants (log β)^a of Mⁿ⁺–DTBA Complexes As Determined Potentiometrically at 25 °C and I = 0.1 M (from KNO₃)^b

	log β _{ijk}				
	MHL	M ₂ H ₃ L ₃	MH ₂ L ₂	MHL ₂	ML ₂
Zn(II)	20.08 ± 0.04	64.73 ± 0.02	39.22 ± 0.02	30.38 ± 0.03	20.30 ± 0.03
Cd(II)	22.60 ± 0.06	71.99 ± 0.04	42.34 ± 0.04	33.22 ± 0.05	^c
Ni(II)	19.25 ± 0.14	63.82 ± 0.06	39.66 ± 0.03	29.72 ± 0.05	17.9 ± 0.2
Co(II)	18.52 ± 0.05	^c	34.6 ± 0.1	25.5 ± 0.1	15.7 ± 0.2
Cu(I)	27.40 ± 0.09	75.2 ± 0.1	43.1 ± 0.1	34.36 ± 0.09	24.2 ± 0.1

^aβ M_iH_jL_k = [M_iH_jL_k]/([M]ⁱ[H]^j[L]^k), where [L] is the concentration of fully deprotonated DTBA. ^bStandard deviations are given as provided by SUPERQUAD calculations.³⁴ ^cStability constant not determined under the applied conditions.

including 0.5 equiv of DTBA_{ox} per Cu(I). The analysis of titration curves revealed that Cu(I) was bound tightly by DTBA already at pH 2.5, which is the initial pH of the titrations. Besides their different affinities for DTBA, all of the metal ions studied exhibited a similar stoichiometric pattern in a wide pH range with small exceptions. The MHL and M₂H₃L₃ complexes were formed at acidic pH and turned into MH₂L₂, MHL₂, and ML₂ species at basic pH (Table 2). For divalent metal ions, exceptions included the absence of the M₂H₃L₃⁺ dimer for Co(II) and the fully deprotonated ML₂²⁻ complex for Cd(II).

The stoichiometries of the most acidic species were also tested by investigating the elemental compositions of precipitates obtained at a 1:2.2 metal/ligand ratio. Complexes were precipitated at various pHs within the 3.5–5.5 range depending on the metal chloride. Solids washed three times and dried at 65 °C were analyzed regarding their C, H, N, and S content. The results, presented in Table S2 (SI), indicate a uniform 1:1 composition, corresponding to a neutral MHLCl species for all of the divalent metal ions. For Cu(I), the elemental analysis matched a Cu₂HLCl stoichiometry. The oligonuclear complexes prepared using metal nitrates or sulfates under identical conditions reflected different elemental compositions, but the differences were due to the presence of a counterion other than chloride (data not shown).

Independent confirmation for pH-dependent complex equilibria provided by potentiometry was obtained by UV–vis spectroscopy. Figure 4 shows the spectra of individual Mⁿ⁺–

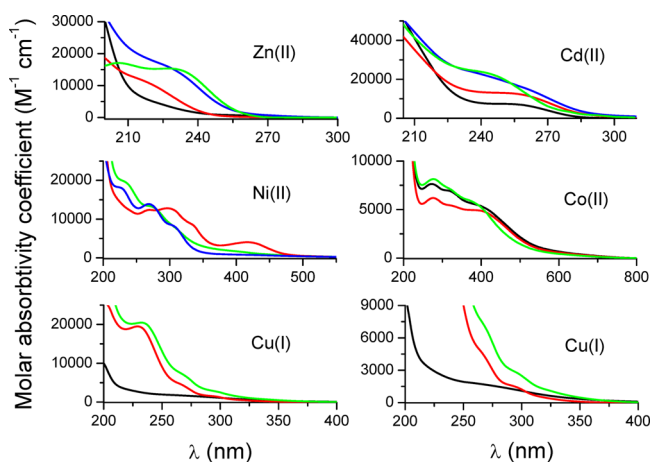


Figure 4. UV–vis spectra of DTBA complexes. The spectra were obtained directly from experiments for complexes approaching 100% abundance (Cd₂H₃L₃, NiH₂L₂, Cu₂H₂L₂) or calculated using speciation data from potentiometry at the concentration used in UV–vis titration. The following colors were used for the corresponding complex species: (black) MHL, (red) M₂H₃L₃, (blue) MH₂L₂, and (green) ML₂. The bottom right graph is an expansion of low intensity features in the Cu(I)–DTBA spectra.

DTBA complexes. These spectra were calculated from the experimental spectra using speciation data derived from potentiometry. They demonstrate charge transfer (CT), d-d, and mixed CT + d-d transitions, depending on the metal ion (see the Discussion for details). Comparison of absorbance values read at characteristic bands or band shoulders with the species distribution diagram, calculated for identical reactant concentrations, confirmed the correctness of the latter (Figure 5). The absorption spectral parameters are presented in Table 3.

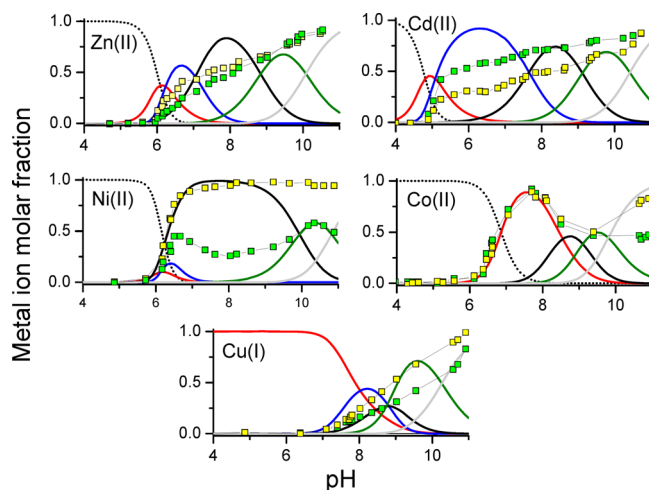


Figure 5. Speciation plots calculated for reactant concentrations used in UV–vis spectroscopic measurements. The following uniform color line styles were used for corresponding metal ion species: (---) Mⁿ⁺, (red) MHL, (blue) M₂H₃L₃, (black) MH₂L₂, (orange) MHL₂, and (gray) ML₂. Free Cu⁺ ions were not present in the pH range shown. The intensities of UV–vis spectra at particular wavelengths were multiplied by the appropriate arbitrary factors to fit the diagrams, with absorption for Zn(II) at 214 nm (yellow squares) and 232 nm (green squares), Cd(II) at 247 nm (yellow squares) and 258 nm (green squares), Ni(II) at 304 nm (yellow squares) and 417 nm (green squares), Co(II) at 390 nm (yellow squares) and 600 nm (green squares), and Cu(I) at 250 nm (yellow squares) and 262 nm (green squares). A 1:4 metal/ligand ratio was used consistently, with overall DTBA concentrations of 300 μM for Cu(I) and 100 μM for the other metal ions.

The diamagnetic complexes of Zn(II), Cd(II), Cu(I), and Ni(II) were also characterized by ¹H NMR spectra, recorded at pH values corresponding to maximum abundances of particular forms. Examples of these spectra are presented in Figure S5 (SI), and the chemical shifts are compared to those of free DTBA in Figure S6 (SI). In all cases, DTBA was in fast exchange between the free and metal-bound states, including Ni(II) complexes, which were in a slow exchange regime with DTT.⁷ All metal ions caused broadening of all signals; however, signals of H^{β'} and H^{γ'}, being the closest to sulfur atoms, broadened the most. In all spectra of the complexes, the signals from DTBA_{ox} were observed at varying intensities, indicating that DTBA oxidation occurred in NMR samples like it did with DTBA alone. The highest extent of oxidation was found for the Ni(II)–DTBA system. The effects of metal ion coordination on the chemical shifts of DTBA protons were minor in most cases.

To characterize the reactivity of complexes of DTBA, we reacted them with DTNB, a model disulfide that is very easily reduced to its thiol monomer yellow TNB ($\epsilon = 14150 \text{ M}^{-1} \text{ cm}^{-1}$ at 412 nm).³² Figure 6 demonstrates the influence of metal ions on the reduction of excess DTNB by 10 μM DTBA. The reaction was monitored for 10 min and clearly occurred in two phases. The rapid phase occurred within 9 s, which was the dead time of the experimental procedure and consumed most of the reacted DTBA. It was followed by a much slower minor process that was apparently completed within 7–10 min. Metal-free DTBA was fully oxidized in the first reaction phase, as was a large proportion of DTBA, being 4-fold excess relative to the metal ions. Oxidation of DTBA in the second phase clearly depended on the stability of the complexes, with Cu(I) and Cd(II) providing much better protection than Zn(II) or

Table 3. UV–Vis Spectroscopic Characterization of Major Complexes of DTBA with Wavelengths of Band Center Given along with Molar Absorptivity Coefficients in Parentheses ($M^{-1} \text{ cm}^{-1}$, Calculated per Mole of Metal Ion)^a

metal ion	MHL	$M_2H_3L_3$	MH_2L_2	ML_2
Zn(II)	sh265 (600) sh220 (6500)	sh270 (650) sh225 (10800)	sh280 (800) sh228 (15600)	sh280 (750) 231 (31500)
Cd(II)	sh250 (8500)	sh248 (14000)	sh234 (24200)	^c
Ni(II)	^b	417 (4050) sh322 (8800) 297 (12750) 269 (12350)	sh303 (8500) 269 (13800) sh225 (18200)	sh390 (1800) sh305 (8200) sh271 (13300) sh230 (19800)
Co(II)	272 (7600) sh316 (9650) sh392 (5440)	^c	^b	277 (8150) 314 (7236) 370 (5950)
Cu(I)	sh350 (350) sh266 (1700) sh218 (3450)	sh320 (450) sh292 (1550) sh264 (4900) 218 (19500)	^b	sh322 (350) sh294 (990)

^aValues were obtained by the comparison of UV–vis spectra with species distributions calculated for concentrations of the reactants used in the titration. ^bParameters of the species not determined due to its low abundance. ^cSpecies not detected in potentiometric experiments.

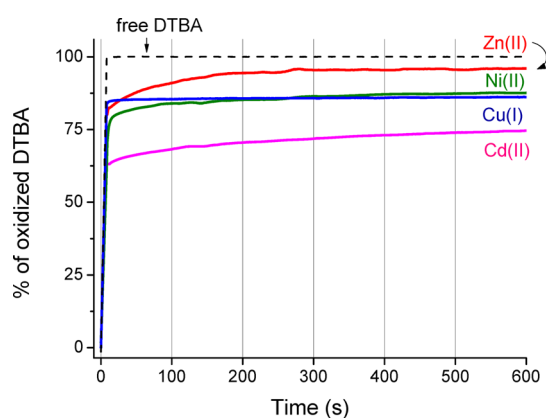


Figure 6. Influence of metal ions on the oxidation of DTBA by DTNB. Freshly prepared $100 \mu\text{M}$ DTNB was mixed with either $10 \mu\text{M}$ DTBA (dashed line) or its complexes, $2.5 \mu\text{M}$ Zn(II), Ni(II), Cd(II), or Cu(I), and incubated for 600 s. The reaction was monitored at 412 nm and recalculated into percentages of oxidized DTBA.

Ni(II). The effect of Co(II) was also tested; however, the reaction kinetics were not consistent with regular kinetic models, indicating the presence of side processes (data not shown).

The reducing ability of DTBA toward protein disulfides was studied in the original report for two enzymes, creatinine kinase and papain, the activities of which were extinguished by modification of their catalytic cysteine residues.¹ A significant difference between DTT and DTBA was observed for the second enzyme, where DTBA yielded more rapid enzyme reactivation. To examine whether metal ions would be able to affect protein reduction by DTBA, we used MMTS-modified papain. Figure 7 shows the influence of individual metal ions on the kinetics of papain reactivation by DTBA and its complexes. Zn(II), Cd(II), and Cu(I) exhibited similar second-order kinetics, as did free DTBA (Figure 7a), whereas Ni(II) and Co(II) demonstrated a more complex reaction (Figure 7b). The kinetic constant k_{obs} , determined for the reactivation of papain by free DTBA, was $7300 \text{ M}^{-1} \text{ s}^{-1}$; the k_{obs} values in complexes with Cu(I), Ni(II), Cd(II), and Zn(II) were slower (Table 4). It should be noted that the k_{obs} for DTBA in the presence of Ni(II) was fitted using only the first four reaction

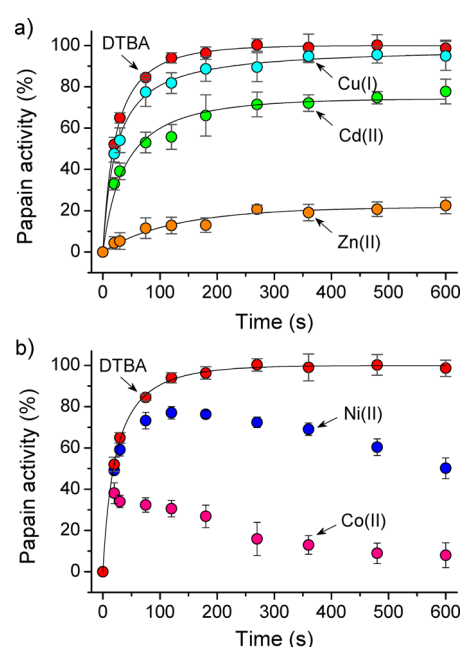


Figure 7. Effects of metal ions on the reactivation of MMTS-modified papain by DTBA. Samples of $50 \mu\text{M}$ MMTS-modified papain were incubated with $100 \mu\text{M}$ DTBA or its complexes (4:1 ligand/metal ratio), and enzyme activity was monitored. (a) Effect of Cu(I), Cd(II), and Zn(II) and (b) effect of Ni(II) and Co(II) (see Experimental Section for details). Red circles represent kinetics of enzyme reactivation by $100 \mu\text{M}$ DTBA, given for comparison. Data were fitted to a second-order rate kinetics equation.

points due to the presence of a secondary deleterious process. Determination of k_{obs} of Co(II)–DTBA enzyme reactivation was not possible for the same reason.

DISCUSSION

Properties of Free DTBA. The combined results of potentiometry, spectropolarimetry, NMR spectroscopy, and UV–vis spectroscopy yielded convergent values for the dissociation constants of DTBA. These results shed light on acid–base properties of the molecule. The $\text{p}K_{\text{a}}$ values of the thiols differ slightly from those reported by Raines and co-

Table 4. Influence of 2.5 μM Metal Ions on the Kinetics of Activation of 5 μM MMTS-Modified Papain by 10 μM DTBA^a

activator	$k_{\text{obs}} \times 10^{-3} \text{ (M}^{-1} \text{ s}^{-1}\text{)}$
DTBA	7.3 ± 0.7
Zn(II)–DTBA	1.7 ± 0.3
Cd(II)–DTBA	5.7 ± 0.7
Ni(II)–DTBA	6.4 ± 0.8^b
Co(II)–DTBA	^c
Cu(I)–DTBA	6.8 ± 0.4

^aActivity of the enzyme was monitored using BAPNA, and k_{obs} values were obtained by data fitting using a previously published formula.¹

^bValue calculated using the first four experimental points. ^cValue not determined due to significant changes in velocity.

workers.¹ The main difference is seen for the $\text{p}K_{\text{a}1}$ value characterizing the thiol group at the β' position. The value of this constant was determined here to be 7.8, which is 0.4 logarithmic unit lower than the previously reported value.¹ The second $\text{p}K_{\text{a}}$ ($\text{p}K_{\text{a}2}$) is identical to the published value. The reason for this difference is the usage of one spectrophotometric titration set in the original report together with data fitting using a different equation that assumes that individual dissociations cannot be discerned and that both deprotonations exert equal effects on the monitored parameter. Careful titration at slightly different wavelengths (233 and 231 nm) allowed us to observe a characteristic inflection point indicative of a significant difference in acidity between the two thiols (Figures S1 and S3, SI). Experimental data were therefore fitted to a two-step binding model, which was convergent with data obtained using other methods. Moreover, the constants determined by potentiometry uncovered a significant separation of the constants, thus excluding a major overlap of both events. Separation of the dissociation events results in very good agreement of the potentiometrically and spectroscopically obtained data (Table 1). This finding indicates that DTBA is even more acidic than previously thought, which is reflected in its unique reducing properties. Figure 2 shows the species distribution of DTBA at a wide range of pHs. At pH 7.0, which is commonly used for the characterization of redox potentials, $\sim 12\%$ of the more acidic thiol is dissociated. At pH 7.4, it is $\sim 25\%$. For comparison, the extent of dissociation of the less basic of the DTT thiols is 0.8% and 1.7% at pH 7.0 and 7.4, respectively.⁷

Higher acidity of the thiols of DTBA makes this disulfide reducing agent much more suitable for application at pHs lower than 7.4 relative to commonly used DTT. This is particularly important when one considers the higher acidity of several cellular compartments, such as endosomes, lysosomes, secretory granules, and the Golgi network. The application of DTBA in biochemical studies at lower pH is therefore more reasonable, especially when almost identical redox potential values of DTT and DTBA are taken into consideration.¹ In this context, it is worthwhile to mention that TCEP, a non-thiol disulfide reducing agent, is very reactive under acidic conditions because its reactivity depends on a single phosphine group characterized by a $\text{p}K_{\text{a}}$ of 7.68.²³

Our experiments also provided a precise value for the dissociation constant of the DTBA amine, which is very basic ($\text{p}K_{\text{a}3} = 10.99$). This high basicity has a critical impact on the acidity of the β' thiol through Coulombic and inductive effects. Similar but slightly lower basicity was observed for the amine

function of cysteamine, which has a similar arrangement of atoms, $\text{SH}-\text{CH}_2-\text{CHR}-\text{NH}_2$ ($\text{p}K_{\text{a}}$ of 10.44).¹⁰ In contrast, oxidation of DTBA to its cyclic form eliminates the thiol groups, which in turn decreases the basicity of the amine group due to the lack of electrostatic interaction between thiolate and a positively charged amine ($-\text{S}^-\cdots\text{H}_3\text{N}^+$). The amine dissociation constant ($\text{p}K_{\text{a}}$) in DTBA_{ox} is more than two logarithmic units lower (8.6) than that of DTBA (Figure S4, SI). Spectrophotometric titration of DTBA at basic pH uncovers a bathochromic shift of thiolate absorption, which is associated with deprotonation of the amine group. This observation confirms an interaction of the β' thiol with the amine group. Interactions of particular groups are also visible in ^1H NMR titrations. For instance, the H^{α} proton closest to the amine group shifts a similar amount upon thiol deprotonation (Figure 3). Likewise, the H^{γ} proton, which is closest to the thiol, also shifts around pH 11 (Table S1, SI). Similar interactions of individual groups occurring through space were observed in reduced and oxidized glutathione molecules.^{36,37}

Complex Formation. The modes of coordination of Ni(II), Cd(II), Co(II), and Zn(II) ions to DTBA exhibited common features. At acidic and neutral pH, all of the metal ions formed strong mono (MHL) complexes with two thiolates of DTBA bound to the central metal ion (Figure 8a). The DTBA

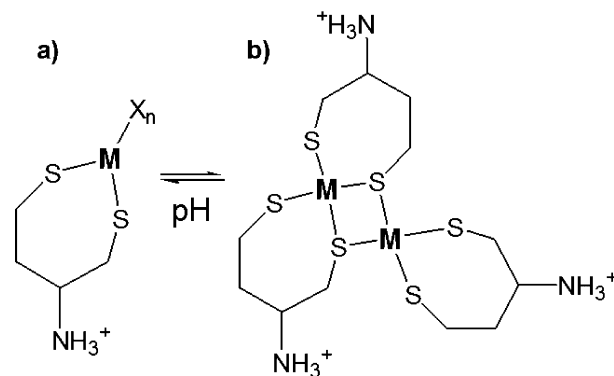


Figure 8. Schematic representation of the structures of (a) MHL and (b) $\text{M}_2\text{H}_3\text{L}_3$ complexes present in weakly acidic pH. X represents water or other molecules bound to metal in the MHL species (e.g., Cl^- for Cu(I)).

complexes differ from their DTT counterparts due to the positively charged amine group of the ligand. Nevertheless, they precipitated from solution in a similar fashion below a 4:1 ligand/metal molar ratio. The composition of these precipitates conformed to the presence of MHL^+ complexes in solution, neutralized with equimolar chloride anions, MHL^+Cl^- (Table S2, SI). These mono complexes remain in equilibrium with the dinuclear $\text{M}_2\text{H}_3\text{L}_3$ complex, which is an intermediate species between 1:1 and 1:2 stoichiometries (Figure 8b). Similar species were observed for DTT, but two such intermediate polynuclear complexes, M_3L_4 and M_2L_3 , were found there. The presence of the $\text{M}_2\text{H}_3\text{L}_3$ complex was confirmed by UV–vis spectra (Figure 4).

The bis (MH_xL_2 , where $x = 2, 1, 0$) complexes of DTBA are predominant in neutral and basic pH for all of the investigated metal ions. UV–vis titrations confirmed the speciation derived from potentiometric titrations, indicating a tetrathiolate coordination mode. Because the amine group demonstrated very high basicity, it did not participate in coordination of the

metal ions. On the basis of this fact, these differently protonated MH_xL_2 complexes are present in a relatively wide range of pHs (Figure 9). The pK_a values obtained from

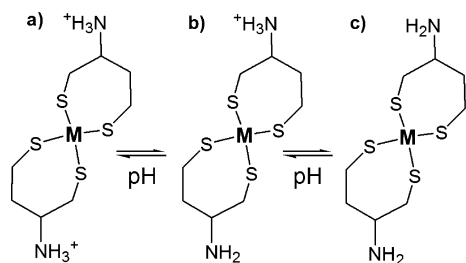


Figure 9. Schematic representation of bis-complex structures relevant at neutral and basic pH: (a) MH_2L_2 , (b) MHL_2 , and (c) ML_2 .

potentiometry vary between 8.7 and 11.8, depending on the metal ion. These values are slightly lower than that of the free DTBA molecule due to electrostatic effects in those complexes, such as a higher overall charge per amine of the dissociating species. This indicates that amine group dissociation is not related to metal binding. UV-vis data (Figure 4) demonstrated that the geometry of MH_2L_2 differs slightly compared to that of MHL_2 and ML_2 , indicating that the charge state of the amine affects the geometry of these complexes to a small extent.

Cu(I) is different for two reasons. First, the Cu(I) complex was found to be present even at pH 2.5, the starting point of our titrations. This behavior demonstrates a very high affinity of Cu(I) for DTBA, similar to the case of DTT. Second, the composition of the precipitate formed by Cu(I) with DTBA at low pH indicated a possible solution structure of the CuHL complex. This complex, unlike those with divalent cations, has neutral charge. Principally, it should retain the same stoichiometry in the solid state. Instead, the minimal stoichiometry of the precipitated complex includes another Cu(I) cation that is neutralized by a chloride anion. This composition strongly suggests that a chloride ion remains bonded to Cu(I) in this complex, which thus has a -1 charge in

solution and collects another Cu(I) for neutralization (Figure 8a). Such trigonal coordination is compatible with known properties of Cu(I) complexes. It occurs because the dithiobutyl chain of DTBA is too short to provide a linear arrangement of thiolate ligands around the Cu(I) ion. The only likely alternative, a dimer composed of two CuHL units, is indistinguishable from the monomer by potentiometry but can be excluded on the basis of the composition of the precipitate (i.e., $Cu_2H_2L_2$ is also neutral and does not need a chloride to be neutralized) and the rather featureless UV spectrum, which suggests the absence of additional interactions between Cu(I) ions and their thiolate ligands. Coordination of chloride to Cu(I) is also supported by the known high affinity of these two ions.^{38,39} Preparation of oligonuclear DTBA complexes using metal nitrates and sulfates reflects different elemental content (elevated N and S content, respectively, data not shown) that demonstrates that anions are required as counterions in the precipitation process.

Mononuclear Cu(I)-thiolate complexes often absorb at around 240–270 nm, and clusters have a band at 300–350 nm.⁴⁰ Spectra presented in Figure 4 that correspond to major complexes absorb above 300 nm with variably pronounced shoulders. This feature suggests an admixture of di-, tri-, and higher polynuclear complexes for Cu(I) in equilibrium. Potentiometry is a quantitative method but only for the definition of thiol acidity. It cannot readily distinguish between ML_2 and M_nL_{2n} complexes, for example, without the support of other techniques. In the case of our data, comparison of potentiometry with absorption data below 300 nm gives good support for the potentiometric model (Figure 5 and Table 3) but cannot exclude the presence of small amounts of polynuclear components.

Ni(II) and Co(II) are respectively d^8 and d^7 ions, thus having metal-centered d-d absorption bands. However, the electronic levels of coordinated thiolates are known to mix with d levels of these metal ions under favorable geometric conditions resulting in band intensities nearly as intense as those of charge transfers (CTs) at wavelengths normally associated with weak d-d

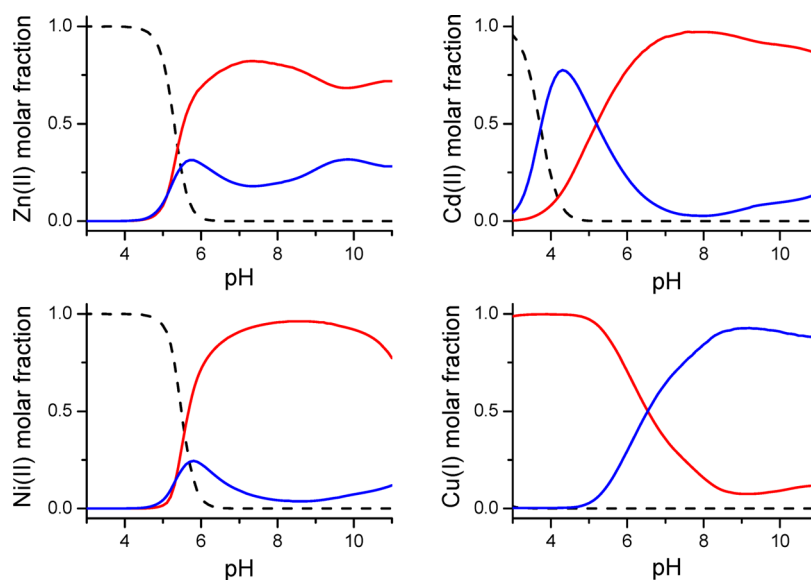


Figure 10. Comparison of metal-binding abilities of DTBA and DTT over a wide range of pHs. Diagrams were calculated for 1 mM DTBA or DTT and 0.5 mM metal ions using stability constants both published previously and determined in this study.⁷ The black dashed, red, and blue lines correspond to free metal ion (M^{2+}), M^{2+} -DTBA, and M^{2+} -DTT, respectively.

electronic transitions. This happens for square-planar Ni(II) thiolate complexes^{7,41–44} and for tetragonal (e.g., square-pyramidal) Co(II) complexes.^{38,45–47} There are no d-d absorption bands at wavelengths longer than 650 nm in the Co(II)–DTBA spectra. Such bands are a fingerprint for tetrahedral Co(II)–thiolate complexes, and their absence indicates that Co(II) formed tetragonal rather than tetrahedral complexes with DTBA.^{48,49} The possibility of a high-spin Ni(II) pyramidal complex is highly unlikely because they are usually formed by sterically constrained ligands. Also, in such complexes, the lowest energy spectral band usually occurs below 500 nm.^{45,46,50} Additionally, aside from broadening, the fact that there was only a very minor impact of the coordinated Ni(II) ions on the ¹H NMR spectra of DTBA and that there was a fast exchange regime strongly supports the binding modes in which flexible DTBA molecules are tethered to the Ni(II) ions solely via sulfur atoms and retain high flexibility due to the absence of steric hindrance.

The Zn(II), Cd(II), and Cu(I) ions are essentially spectroscopically silent, being d¹⁰ ions, but CT transitions are present in the spectra of thiolate complexes of these ions.^{7,15,25,28,51–54} The positions and intensities of the CT bands for Zn(II), Cd(II), and Cu(I) are similar to those of previously characterized ZnS₄, CdS₄, and CuS₄ coordination types seen for DTT complexes^{7,20} and for biologically relevant thiolate ligands, such as zinc fingers,^{24–28} metallothioneins,^{15,55,56} phytochelatin,^{51,57,58} and low molecular weight thiols (e.g., glutathione).^{11,59,60} Similarly to Ni(II)–DTBA complexes, Zn(II)–, Cd(II)–, and Cu(I)–DTBA complexes demonstrate high coordination dynamics on the basis of a lack of additional signals observed in the ¹H NMR spectra (Figure S5, SI).

Applications. Comparing the metal-binding abilities of DTBA with DTT on the basis of their log β values determined potentiometrically (Table 1 and 2) showed that, despite structural similarity, they demonstrate significantly different capabilities in metal ion binding. Figure 10 shows that Zn(II) and Ni(II) are bound more tightly by DTBA than DTT throughout the pH range. However, Cd(II) and Cu(I) demonstrate higher affinity for DTBA at basic and acidic pHs, respectively. This observation is confirmed by competitiveness index (CI) calculations of CI_{7.4} values, which are calculated at pH 7.4. The CI_{7.4} values provide a means of comparing metal-binding affinities of complexes having different stoichiometries.¹² These values are presented in Table 5.

Table 5. Competitiveness Index¹² Values for Various Metal Ions with the Disulfide Reductants DTBA and DTT⁷ at pH 7.4, 25 °C, and I = 0.1 M (CI_{7.4})^a

metal ion	DTBA	DTT
Zn(II)	9.166	7.894
Cd(II)	12.532	9.00
Pb(II)	<i>b</i>	9.69
Ni(II)	9.519	6.47
Co(II)	4.912	<i>b</i>
Cu(I)	14.21	14.78

^aCI is the logarithm of the conditional stability constant of MZ (the metal complex of theoretical molecule Z), such that [MZ] = $\sum_{ijkl} [M_i H_j L_k A_l]$, at a given overall component concentration. The concentration of disulfide reductants and Z were set at 0.001 M, and those of the metal ions at 0.00025 M. ^bNo data available in the literature.

Only Cu(I) binds to DTT slightly stronger than to DTBA. The main reason DTBA complexes have elevated stability relative to that of DTT complexes is the positively charged amine group, which causes a reduction in pK_a values of thiols in the ligand molecule, making them more prone to metal ion-dependent deprotonation. This effect is less important for Cu(I) coordination, which is driven by the very high stability of the Cu–S bonds and is thus relatively less susceptible to differences in pK_a values.³¹

Certainly, the high affinity of DTBA for metal ions is a major disadvantage of this new disulfide reducing agent. Moreover, it is common knowledge that application of DTT to immobilized metal ion chromatography (IMAC) frequently results in binding (transfer) of the metal ion from the resin, resulting in decreased protein binding capacity and precipitation of Mⁿ⁺–DTT complexes inside the column. On the basis of the higher affinity of DTBA for metal ions, we expect an even more significant influence of the reductant on IMAC and equilibration with metalloproteins. In our previous report devoted to the coordination properties of TCEP, we showed that this disulfide reducing agent possesses a very low capacity for metal ion chelation, making it an agent of choice for the protection of metalloproteins and metal-binding peptides.²³ Among all of the discussed thiol group protectants, DTBA has the highest affinity for metal ions, whereas TCEP is the most nonbinding molecule. Figure S7 (SI) compares the binding capabilities of TCEP, DTT, and DTBA toward Zn(II), Cd(II), and Ni(II), all metal ions previously studied potentiometrically.^{7,23} For instance, TCEP complexation of Zn(II) is 5.3 and 6.0 orders of magnitude weaker than those of DTT and DTBA, respectively.

High metal affinity is also reflected in reducing properties toward disulfide targets. Addition of any of the investigated metal ions, excluding Co(II), slowed DTNB reduction (Figure 6). Interestingly, this effect correlates very well with the CI_{7.4} values of the DTBA complexes (Figure 11). Zn(II) and Ni(II)

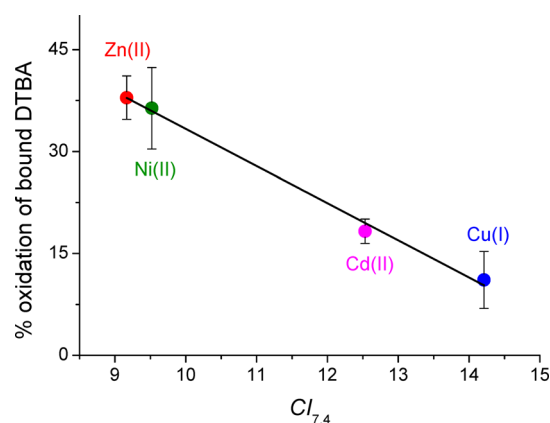


Figure 11. Linear correlation among the overall affinities of DTBA complexes at pH 7.4, represented by CI_{7.4}, and their abilities to protect DTBA from oxidation by DTNB.

demonstrate the lowest and comparable effects on DTNB reduction, respectively, whereas Cu(I) eliminated redox activity of DTBA almost completely. The latter effect is due to the formation of extremely highly stable Cu(I)–DTBA complexes, wherein DTBA thiols are not accessible for exchange with disulfides such as DTNB.

The influence of metal ions on the reduction of MMTS-modified papain with DTBA contrasts the effects observed for the reaction with DTNB. For instance, the Zn(II)–DTBA complex was least efficient at reactivating the oxidized enzyme compared to free DTBA (Table 4). The Cd(II)–DTBA complex, despite its higher thermodynamic stability, reduced the oxidized enzyme 3.3-fold faster than the weaker Zn(II) complex. A similar tendency was observed at the beginning of the reactions with Ni(II) and Co(II) complexes; however, they subsequently caused unspecific inhibition of the enzyme (Figure 7). The active site of papain has an anionic character, and it has been shown previously that DTBA, thanks to its positively charged amine group, can reduce oxidized papain 14-fold faster than neutral DTT.^{1,61,62} The net charge of Cd(II)–, Ni(II)–, and Co(II)–DTBA complexes calculated for the reaction conditions is much more positive than that of Zn(II)–DTBA complexes. The Cu(I)–DTBA species, which has a different stoichiometry at the same pH, marginally slowed the reactivation of MMTS-papain, although the net charge was almost neutral. This is probably due to a stereospecific effect rather than a simple electrostatic interaction; this interesting issue should be explored further in the future.

As presented above, the unique acidity of DTBA thiols is the consequence of the presence of a positively charged amine group. The high basicity of thiols in DTT confirms this conclusion. Using DTBA for the production of disulfide reducing resin requires usage of the amino group during immobilization.² Consequently, this reaction deprives the DTBA molecule of its positive charge. We expect that immobilized DTBA will have reducing properties similar to those of DTT. To maintain the reducing capabilities of the DTBA resin, another DTBA derivative with an additional function for conjugation should be used.

DTT was recently applied as a competitive agent to determine the Cu(I) binding constants of cellular copper chaperones using electrospray mass spectrometry.^{30,31} This application is based on the assumption that actual concentrations of rather unstable DTT in studied reaction mixtures are independently known, because there is no way to quantify neutral molecules of protonated DTT and its cyclic disulfide DTT_{ox} by mass spectrometry. Also, because of the very high Cu(I) affinities of these proteins, enormous DTT concentrations had to be used. This brings about the possibility that artifacts resulting from ionization quenching by DTT may distort quantitation of Cu(I) transfer from the studied protein to the competitor. DTBA potentially allows one to avoid all of these issues on the basis of its charged amine group and higher metal affinity. Its application could be extended to other physiologically or toxicologically relevant metal cations, including those studied in our work.

CONCLUSIONS

The results presented here demonstrate that DTBA, a novel dithiol reducing agent, is a very strong and versatile metal ion binding agent for all of the metal ions tested, including Zn(II), Cd(II), Ni(II), Co(II), and Cu(I), forming both mononuclear and dinuclear complexes. The stabilities of the DTBA complexes are similar to, or usually even somewhat higher than, those of DTT, limiting its usage. The strong reducing abilities of DTBA depend on the very basic amine function; thus its neutralization (e.g., by immobilization) should be avoided. Our results demonstrate that metal ions reduce the capability of DTBA to reduce low molecular disulfide DTNB

due to its metal-binding abilities and also affect reactivation of oxidized papain due to stereospecific and electrostatic effects. On the other hand, strong metal-binding abilities can be expected to make DTBA a useful competitive ligand for ESI-MS studies of metal ion affinities to proteins.

ASSOCIATED CONTENT

Supporting Information

UV–vis and ¹H NMR titrations of DTBA, ¹H NMR spectra of DTBA complexes, ¹H NMR of DTBA_{ox}, and metal-binding abilities of DTBA, DTT, and TCEP. This material is available free of charge via the Internet at <http://pubs.acs.org>.

AUTHOR INFORMATION

Corresponding Author

*E-mail: krezel@biotech.uni.wroc.pl

Notes

The authors declare no competing financial interest.

ACKNOWLEDGMENTS

This work was supported by Ministry of Science and Higher Education (MNiSW) Grant IP2012 018272 and partially funded by National Science Centre (NCN) Grant 2012/07/E/NZ1/01894. Instrumentation, J.A., and A.K. were supported by the Polish Foundation for Science under Focus Project F1/2010/P/2013.

REFERENCES

- (1) Lukesh, J. C., 3rd; Palte, M. J.; Raines, R. T. *J. Am. Chem. Soc.* **2012**, *134*, 4057–4059.
- (2) Lukesh, J. C., 3rd; Vanveller, B.; Raines, R. T. *Angew. Chem., Int. Ed.* **2013**, *52*, 12901–12904.
- (3) Cleland, W. W. *Biochemistry* **1964**, *3*, 480–482.
- (4) Burns, J. A.; Butler, J. C.; Moran, J.; Whitesides, G. M. *J. Org. Chem.* **1991**, *56*, 2648–2650.
- (5) Whitesides, G. M.; Lamoureux, G. V. *J. Org. Chem.* **1993**, *58*, 633–641.
- (6) Owen, L. N.; Smith, P. N. *J. Chem. Soc.* **1951**, 2973–2975.
- (7) Krężel, A.; Leśniak, W.; Jeżowska-Bojczuk, M.; Młynarz, P.; Brasuń, J.; Kozłowski, H.; Bal, W. *J. Inorg. Biochem.* **2001**, *84*, 77–88.
- (8) Lamoureux, G. V.; Whitesides, G. M. *J. Org. Chem.* **1993**, *58*, 633–641.
- (9) Loechler, E. L.; Hollocher, T. C. *J. Am. Chem. Soc.* **1980**, *102*, 7312–7321.
- (10) Connett, P. H.; Wetterhahn, K. E. *J. Am. Chem. Soc.* **1986**, *108*, 1842–1847.
- (11) Krężel, A.; Bal, W. *Bioinorg. Chem. Appl.* **2004**, 293–305.
- (12) Krężel, A.; Wójcik, J.; Maciejczyk, M.; Bal, W. *Chem. Commun. (Cambridge, U.K.)* **2003**, 704–705.
- (13) Collet, J. F.; D'Souza, J. C.; Jakob, U.; Bardwell, J. C. *J. Biol. Chem.* **2003**, *278*, 45325–45332.
- (14) Maret, W.; Vallee, B. L. *Proc. Natl. Acad. Sci. U.S.A.* **1998**, *95*, 3478–3482.
- (15) Krężel, A.; Maret, W. *J. Am. Chem. Soc.* **2007**, *129*, 10911–10921.
- (16) Kurowska, E.; Sasin-Kurowska, J.; Bonna, A.; Grynberg, M.; Poznański, J.; Knizewski, L.; Ginalski, K.; Bal, W. *Metallomics* **2011**, *3*, 1227–1231.
- (17) Witkiewicz-Kucharczyk, A.; Bal, W. *Toxicol. Lett.* **2006**, *162*, 29–42.
- (18) Van Kerkhove, E.; Pennemans, V.; Swennen, Q. *BioMetals* **2010**, *23*, 823–855.
- (19) Fricker, S. P. *Metallomics* **2010**, *2*, 366–377.
- (20) Cornell, N. W.; Crivaro, K. E. *Anal. Biochem.* **1972**, *47*, 203–211.

- (21) Po, H. N.; Legg, K. D.; Kuwahara, S. S. *Anal. Lett.* **1973**, *6*, 659–661.
- (22) Gnonlonfon, N.; Filella, M.; Berthon, G. *J. Inorg. Biochem.* **1991**, *42*, 207–215.
- (23) Krężel, A.; Latajka, R.; Bujacz, G. D.; Bal, W. *Inorg. Chem.* **2003**, *42*, 1994–2003.
- (24) Miłoch, A.; Krężel, A. *Metallomics* **2014**, *6*, 2015–2024.
- (25) Sénéque, O.; Latour, J. M. *J. Am. Chem. Soc.* **2010**, *132*, 17760–17774.
- (26) Sikorska, M.; Krężel, A.; Otlewski, J. *J. Inorg. Biochem.* **2012**, *115*, 28–35.
- (27) Bal, W.; Schwerdtle, T.; Hartwig, A. *Chem. Res. Toxicol.* **2003**, *16*, 242–248.
- (28) Kochańczyk, T.; Jakimowicz, P.; Krężel, A. *Chem. Commun. (Cambridge, U.K.)* **2013**, *49*, 1312–1314.
- (29) Wang, Z.; Rejtar, T.; Zhou, Z. S.; Karger, B. L. *Rapid Commun. Mass Spectrom.* **2010**, *24*, 267–275.
- (30) Banci, L.; Bertini, I.; Ciofi-Baffoni, S.; Leontari, I.; Martinelli, M.; Palumaa, P.; Sillard, R.; Wang, S. L. *Proc. Natl. Acad. Sci. U.S.A.* **2007**, *104*, 15–20.
- (31) Banci, L.; Bertini, I.; Ciofi-Baffoni, S.; Kozyreva, T.; Zovo, K.; Palumaa, P. *Nature* **2010**, *465*, 645–648.
- (32) Eyer, P.; Worek, F.; Kiderlen, D.; Sinko, G.; Stuglin, A.; Simeon-Rudolf, V.; Reiner, E. *Anal. Biochem.* **2003**, *312*, 224–227.
- (33) Irving, H.; Miles, M. G.; Pettit, L. D. *Anal. Chim. Acta* **1967**, *38*, 475–488.
- (34) Gans, P.; Sabatini, A.; Vacca, A. *J. Chem. Soc., Dalton Trans.* **1985**, 1195–1199.
- (35) Krężel, A.; Bal, W. *J. Inorg. Biochem.* **2004**, *98*, 161–166.
- (36) Krężel, A.; Bal, W. *Org. Biomol. Chem.* **2003**, *1*, 3885–3890.
- (37) Krężel, A.; Wójcik, J.; Maciejczyk, M.; Bal, W. *Inorg. Chem.* **2011**, *50*, 72–85.
- (38) Fritz, J. J. *J. Phys. Chem.* **1984**, *88*, 4358–4361.
- (39) Xiao, Z.; Gammons, C. H.; Williams-Jones, A. E. *Geochim. Cosmochim. Acta* **1998**, *62*, 2949–2964.
- (40) Pujol, A. M.; Gateau, C.; Lebrun, C.; Delangle, P. *J. Am. Chem. Soc.* **2009**, *131*, 6928–6929.
- (41) Lever, A. B. P. *Inorganic Electronic Spectroscopy*, 2nd ed.; Elsevier: New York, 1984.
- (42) Colpas, G. J.; Kumar, M.; Day, R. O.; Maroney, M. J. *Inorg. Chem.* **1990**, *29*, 4779–4788.
- (43) Maroney, M. J.; Choudhury, S. B.; Bryngelson, P. A.; Mirza, S. A.; Sherrod, M. J. *Inorg. Chem.* **1996**, *35*, 1073–1076.
- (44) Jenkins, R. M.; Singleton, M. L.; Almaraz, E.; Reibenspies, J. H.; Darensbourg, M. Y. *Inorg. Chem.* **2009**, *48*, 7280–7293.
- (45) Harding, D. J.; Harding, P.; Dokmaisrijan, S.; Adams, H. *Dalton Trans.* **2011**, *40*, 1313–1321.
- (46) Fujisawa, K.; Kakizaki, T.; Miyashita, Y.; Okamoto, K. *Inorg. Chim. Acta* **2008**, *361*, 1134–1141.
- (47) Desrochers, P. J.; Cutts, R. W.; Rice, P. K.; Golden, M. L.; Graham, J. B.; Barclay, T. M.; Cordes, A. W. *Inorg. Chem.* **1999**, *38*, 5690–5694.
- (48) Bertini, I.; Luchinat, C. *Adv. Inorg. Biochem.* **1984**, *6*, 71–111.
- (49) Krizek, B. A.; Merkle, D. L.; Berg, J. M. *Inorg. Chem.* **1993**, *32*, 937–940.
- (50) Jacobsen, F. E.; Breece, R. M.; Myers, W. K.; Tierney, D. L.; Cohen, S. M. *Inorg. Chem.* **2006**, *45*, 7306–7315.
- (51) Dorčák, V.; Krężel, A. *Dalton Trans.* **2003**, 2253–2259.
- (52) Heinz, U.; Kiefer, M.; Tholey, A.; Adolph, H. W. *J. Biol. Chem.* **2005**, *280* (5), 3197–3207.
- (53) Imriskova-Sosova, I.; Andrews, D.; Yam, K.; Davidson, D.; Yachnin, B.; Hill, B. C. *Biochemistry* **2005**, *44*, 16949–16956.
- (54) Doku, R. T.; Park, G.; Wheeler, K. E.; Splan, K. E. *J. Biol. Inorg. Chem.* **2013**, *18*, 669–678.
- (55) Freisinger, E.; Vašák, M. *Met. Ions Life Sci.* **2013**, *11*, 339–371.
- (56) Meloni, G.; Zovo, K.; Kazantseva, J.; Palumaa, P.; Vasák, M. *J. Biol. Chem.* **2006**, *281* (21), 14588–14595.
- (57) Mehra, R. K.; Mulchandani, P. *Biochem. J.* **1995**, *307*, 697–705.
- (58) Kobayashi, R.; Yoshimura, E. *Biol. Trace Elem. Res.* **2006**, *114*, 313–318.
- (59) Krężel, A.; Bal, W. *Acta Biochim. Pol.* **1999**, *46*, 567–580.
- (60) Mah, V.; Jalilehvand, F. *JBIC, J. Biol. Inorg. Chem.* **2010**, *15*, 441–458.
- (61) Schechter, I.; Berger, A. *Biochem. Biophys. Res. Commun.* **1967**, *27*, 157–162.
- (62) Pickersgill, R. W.; Harris, G. W.; Garman, E. *Acta Crystallogr., Sect. B* **1992**, *48*, 59–67.